Kubo Lineshape and its Fitted q-Gaussian Tsallis Function

International Journal of Sciences

Research Article Volume 13 – January 2024 (01)

Kubo Lineshape and its Fitted q-Gaussian Tsallis Function

Amelia Carolina Sparavigna[1]

[1]Department of Applied Science and Technology, Polytechnic University of Turin, Italy

Abstract – Here we consider the Kubo lineshape, that is the Fourier transform of Kubo stochastic time-correlation function, and its fitted q-Gaussian function. In particular we investigate how q-Tsallis Gaussian functions can be used as a substitute of a Kubo lineshape. In fact, the q-Gaussian has a simple analytic expression, whereas the Kubo lineshape requires a numerical calculation of Fourier transform. The aim of this investigation is to further generalize the application of q-Gaussian Tsallis functions in Raman spectroscopy.

Keywords: Raman spectroscopy, q-Gaussian Tsallis lines, Time correlation functions, WolframAlpha by Wolfram Research

In a discussion about the Q(5) Raman line of Carbon Monoxide and the generalization of the Voigt function, a function which is widely used in spectroscopy, we have encountered the "Kubo lineshape", that is the Fourier transform of the Kubo (Gaussian-stochastic) time-correlation function. Here we compare the Kubo lineshape with the q-Gaussian Tsallis function. Tsallis q-Gaussians are quite useful for fitting band profiles in Raman spectroscopy, as shown by the many examples provided by us (Sparavigna, 2023). The Tsallis function is a probability distribution derived in a statistical framework (Tsallis, 1988, 1995, Hanel et al., 2009). It consists in a generalized form of the exponential function (see discussion in Sparavigna, 2022), characterized by a continuous parameter q in the range $1 < q < 3$. As given by Umarov et al., 2008, the q-Gaussian is a function $f(x) = Ce_q(-\beta x^2)$, where $e_q(.)$ is the q-exponential function and C a constant. The q-exponential has expression:

$$exp_q(u) = [1 + (1 - q)u]^{1/(1-q)} .$$

The function $f(x)$ possesses a bell-shaped profile, and in the case that we have the peak at position x_o, the q-Gaussian is:

$$\text{q-Gaussian} = Cexp_q(-\beta(x - x_o)^2) =$$

$$C[1 - (1 - q)\beta(x - x_o)^2]^{1/(1-q)}$$

For q equal to 2, the q-Gaussian is the Cauchy-Lorentzian distribution (Naudts, 2009). For q close to 1, the q-Gaussian is a Gaussian. Consequently, for the q-parameter between 1 and 2, the shape of the q-Gaussian function is intermediate between Gaussian and Lorentzian profiles.

As previously shown, q-Gaussian functions can be used to mimic the Voigt convolutions, but they are different functions, in particular for what is regarding the behavior of the wings. The Voigt function, as told by Townsend, 2008, "looks like Gaussian for small *x* (i.e., near line center), and like Lorentzian for large *x* (i.e., out in line wings)". We can also appreciate the same by observing the pseudo-Voigt function, which is generally used for approximating the Voigt function (Meier, 2005). Being the pseudo-Voigt the linear combination of Gaussian and Lorentzian functions, the wings must be necessarily Lorentzian and the kernel Gaussian-like. Consequently, if we use Voigt functions or pseudo-Voigt functions for fitting spectra, the wings of the Raman lines will be always described by a Lorentzian behavior. However, is this always the experimental case? That is, are we always observing Lorentzian wings for the Raman bands? To answer these questions, we started investigation in ChemRxiv1. We observed that a generalization of the pseudo-Voigt functions obtained by means of a linear combination of two q-Gaussians can help us in describing the leading term of the line wings. In this manner, we can quantitatively "measure" the wing power law as well as answering qualitatively whether it is Lorentzian or not. The q-Gaussians are therefore the proper solution for investigation.

For the spectra previously considered (Sparavigna, 2023), the fitted functions are successfully in several cases, for instance graphite ChemRxiv2, anatase ChemRxiv3, SERS spectra ChemRxiv4, and so on, SSRN. In the discussion previously mentioned about the Q(5) line, we considered deeply the Voigt function, its time-correlation functions, and several other time-correlation functions used for spectroscopy. Among them, let us here remember the time correlation producing the Egelstaff-Schofield (ES) lineshape. The ES profiles can be obtained from a Fourier transform which is giving an analytical expression (Kirillov, 1999). In our comparison of ES profiles with q-

Published at: http://www.ijsciences.com/pub/issue/2024-01/
DOI: 10.18483/ijSci.2742; Online ISSN: 2305-3925; Print ISSN: 2410-4477

Amelia Carolina Sparavigna (Correspondence)
+

Gaussians, we noted that the fitted Tsallis function is in good agreement with ES functions.

The ES time-correlation function is (Kirillov, 1999):

$$\Phi(t) = exp\{-[(t^2 + \tau_1^2)^{1/2} - \tau_1]/\tau_2\}. \quad (1)$$

It is containing two relaxation times. According to Kirillov, 1999, we have this function becoming Gaussian for $t \ll \tau_1$ and an exponential for $t \gg \tau_1$. In Kirillov, 1999, 2004, it is stressed that the ES time-correlation function (1) is a function with is able of reproducing the Kubo time-correlation function, in a form possessing an analytic expression of the Fourier transform. And also: the "Gaussian–Markovian, or Kubo case remains the most common and widely used in spectroscopic practice" (Kirillov, 2009). The Kubo correlation is given by Kirillov as (M_2 is the second spectral moment and τ_ω a relaxation time):

$$\Phi = exp\{-M_2\tau_\omega^2[exp(-t/\tau_\omega) - 1 + t/\tau_\omega]\} \quad (2)$$

Here the frequency is referred to the position of the unshifted frequency. "When the frequency modulation is a Gaussian Markov stationary process, [that is, in the Kubo case] the cumulant beyond the second order vanishes" (Dutta et al., 2017). Note please that the time correlation has an exponential factor, which is the Fourier transform of a Lorentzian function:

$$\Phi = exp\{-M_2\tau_\omega t\} \cdot exp\{M_2\tau_\omega^2[1 - exp(-t/\tau_\omega)]\}. \quad (3)$$

That is, we have the system subjected to homogeneous broadening mechanisms.

Kirillov's research considered also the approach defined as Rothschild-Kubo (Rothschild et al., 1987, Feng and Wilde, 1988). "Efforts to apply a simple Gauss-Markov theory have proven unsuccessful for aqueous ionic solutions, where strong Coulombic and dipolar forces promote vibrational relaxation, and the hydrogen bonding of the water inhibits anion reorientation. An alternate modeling function, the stretched exponential, has been proposed to explain inhomogeneously broadened Raman spectra" (Feng & Wilde, 1988). Rothschild et al., 1987, wrote the time correlation related to the stretched exponential as:

$$\Phi = exp\left(-M_2T^2\sum_{n=0}^{\infty}\frac{(-1)^n(t/T)^{2+n\alpha}}{n!\,(1+n\alpha)(2+n\alpha)}\right) \quad (4)$$

(with T instead of τ_ω). Rothschild and coworkers tell the following. "It has by now been generally accepted that the shapes and widths of band profiles observed by vibrational spectroscopy of condensed-phase systems are, in the vast majority of cases, caused by "inhomogeneous broadening. … Although spectral profiles of a large variety of liquid-phase systems have since long been satisfactorily explained by this simple Gauss-Markov process … , more recent and improved spectral data have led to the realization that the experimental vibrational correlation decay in the intermediate to long time domains is occasionally faster (more "Gaussian-like") than predicted by [the Gauss-Markov approach]". In Kirillov, 2004, we can find the Rothschild-Perrot-Guillaume (RPG) model as in Eq.(4), discussed with the Burshtein-Fedorenko-Pusep (BFP) model too.

"Differences in TCFs [time correlation functions] lead to very unlike line profiles. … the Kubo TCF corresponds to vibrational lines whose profiles vary from Gaussian to Lorentzian. The Rothschild-Perrot-Guillaume TCF corresponds to vibrational lines of quite specific, over-Gaussian form. They are less sharp than Gaussian in their central part, and much faster fall to zero in the wings. The Burshtein, Fedorenko and Pusep TCF corresponds to over-Lorentzian line profiles. They are sharper than true Lorentzians in their central part, and broader in the wings" (Kirillov, 2004). Therefore, we can tell that Kirillov is proposing a generalization of the Kubo correlation function.

To use (4) in spectroscopy, we need its Fourier transform to determine the corresponding line profile. Being the Fourier transform calculation too heavy for Raman bands deconvolution, Tagliaferro et al., 2020, have proposed a synthetic profile mimicking the line shape. It is a profile named "GauLor", which is a piecewise symmetric function with a Lorentzian central part and wings which are Gaussians; actually, it seems being the opposite of the Voigt profile (Gaussian central part and Lorentzian wings). In GauLors, the onset of the wing happens at a frequency threshold, determined by the overall fitting approach. At the threshold, the Lorentzian and Gaussian piece functions and their derivatives are continuous. Supposing the existence of the threshold within the Raman scan range, the GauLor has the onset of the Gaussian wing which can be very close to the center of the line (in the kernel) or quite far from it (in the far line wings). In fact, we have two families of intermediate functions between Lorentzian and Gaussian line shapes, and they are the q-Gaussians and the GauLors.

In this framework, with the aim of further generalization to the RPG case, let us consider the q-Gaussian fit of Kubo lines.

The Kubo line shape

Let us consider specifically the Kubo case in the form (super-exponential):

$$\Phi = exp\{-[exp(-t) - 1 + t]\}, \quad (5)$$

We use here a dimensionless time. To show the related line shape we need the Fourier transform. To have it, we can pass through the Laplace transform. Here some screenshots from Wolfram Alpha:

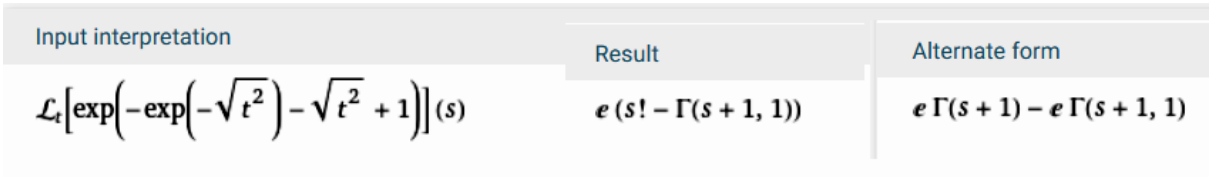

Passing from *s* to *i w* and evaluating the real part, we have the Fourier transform as:

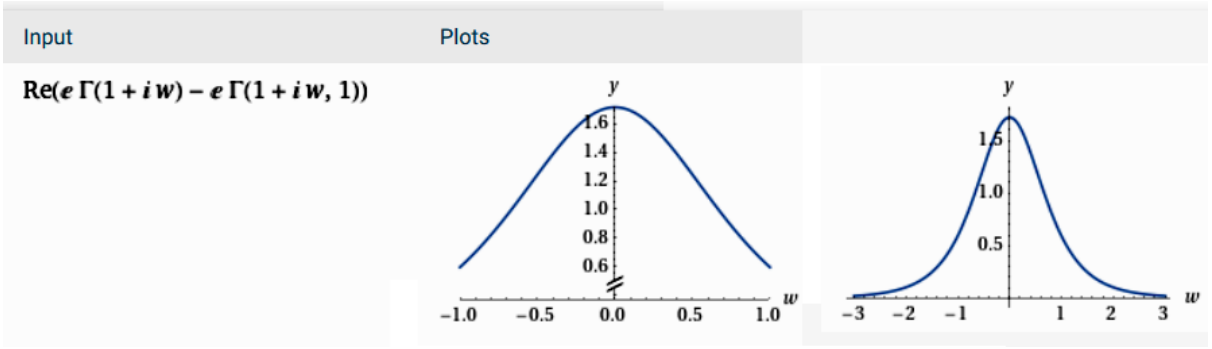

From the table of values of the function, we find the following line shape in linear and semi log scale.

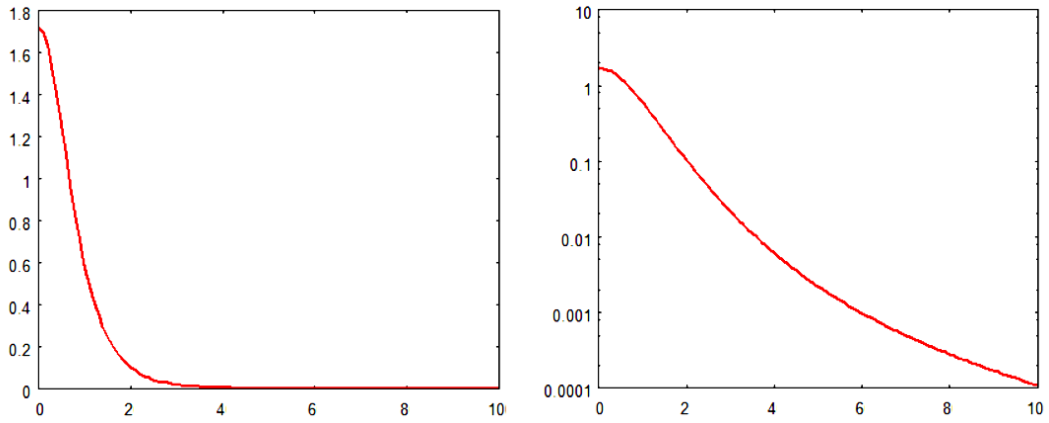

Fig.1: Behavior of the Kubo line shape in linear and semi log scale. Being symmetric, only one side of the profile is shown.

We used the WolframAlpha (WA) data given in the Figure 1, to calibrate the numerical Fourier transform of the time correlation function.

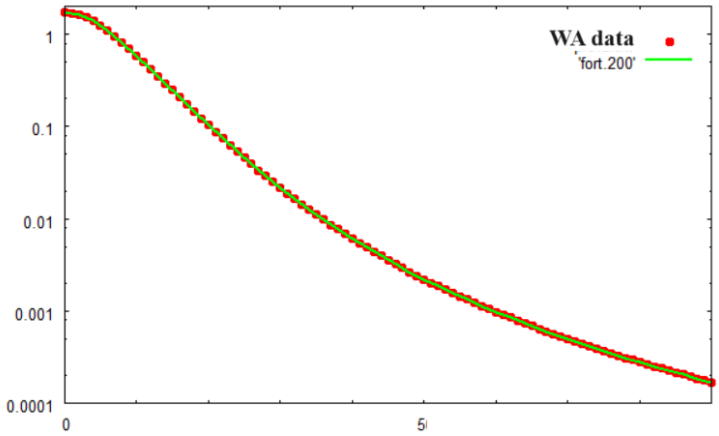

Fig. 2: In red the WolframAlpha data and in green the corresponding numerical Fourier transform.

In the Lecture Notes by Tokmakoff, 2009, the Kubo time correlation function is given as:

$$F(t) = exp[-\Delta^2\tau_c^2(exp(-t/\tau_c) + t/\tau_c - 1)] \quad (6)$$

where τ_c is the time scale of dynamics. Parameter $\kappa = \Delta \cdot \tau_c$ is introduced, and three cases are given: fast, $\Delta = 1, \tau_c = 0.2, \kappa = 0.2$, mid, $\Delta = 1, \tau_c = 1, \kappa = 1$, and slow $\Delta = 1, \tau_c = 10, \kappa = 10$. The corresponding absorption lineshapes are given by Tokmakoff as in the following plot (Fig.3).

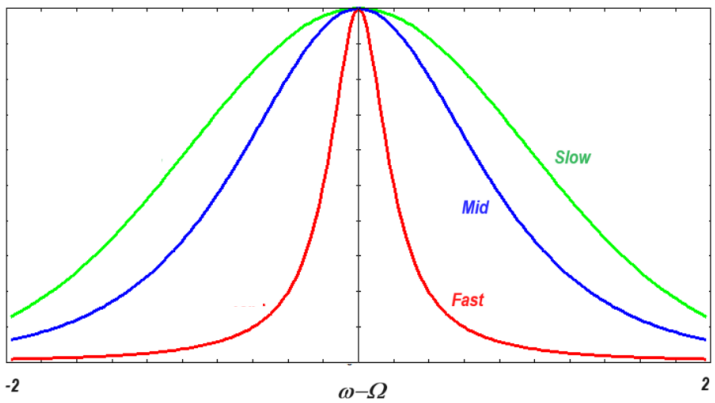

Fig.3.

"We see that for a fixed distribution of frequencies Δ the effect of increasing the time scale of fluctuations through this distribution (decreasing τ_c) is to gradually narrow the observed lineshape from a Gaussian distribution of static frequencies with width (FWHM [Full width at half maximum]) of $2.35 \cdot \Delta$ to a motionally narrowed Lorentzian line shape with width (FWHM) of $\Delta^2 \tau_c/\pi = \Delta \cdot \kappa/\pi$." (Tokmakoff, 2009).

Here again we are facing the problem to find the "intermediate" function between Lorentzian and Gaussian profiles.

We have shown previously that the q-Gaussians are able of mimicking the ES line shape. Let us evaluate how they fit the Kubo line shapes. Here in the following plots, five Kubo profiles are given with different τ_c, κ parameters.

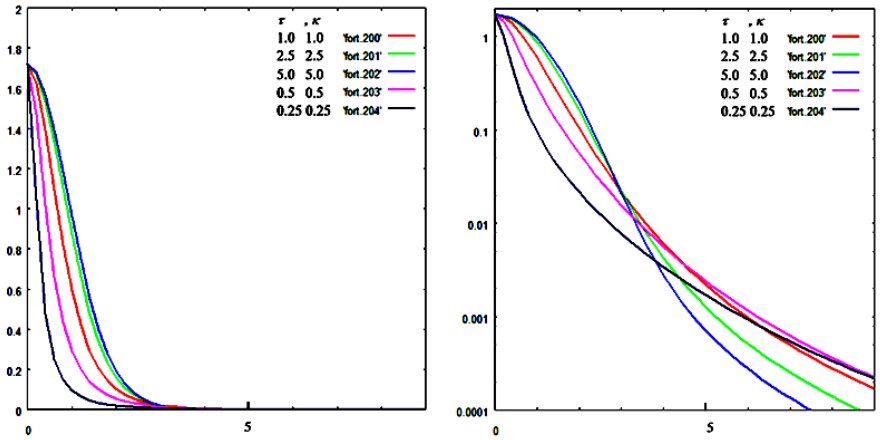

Fig.4: Five Kubo line shapes for different parameters κ, τ_c . In red the mid case $\Delta = 1, \tau_c = 1, \kappa = 1$.

Considering the Kubo lineshapes given in the Figure 4, we compare them with q-Gaussian functions. In the following Figure 5, we can see the Kubo data and the fitted q-Gaussians (green).

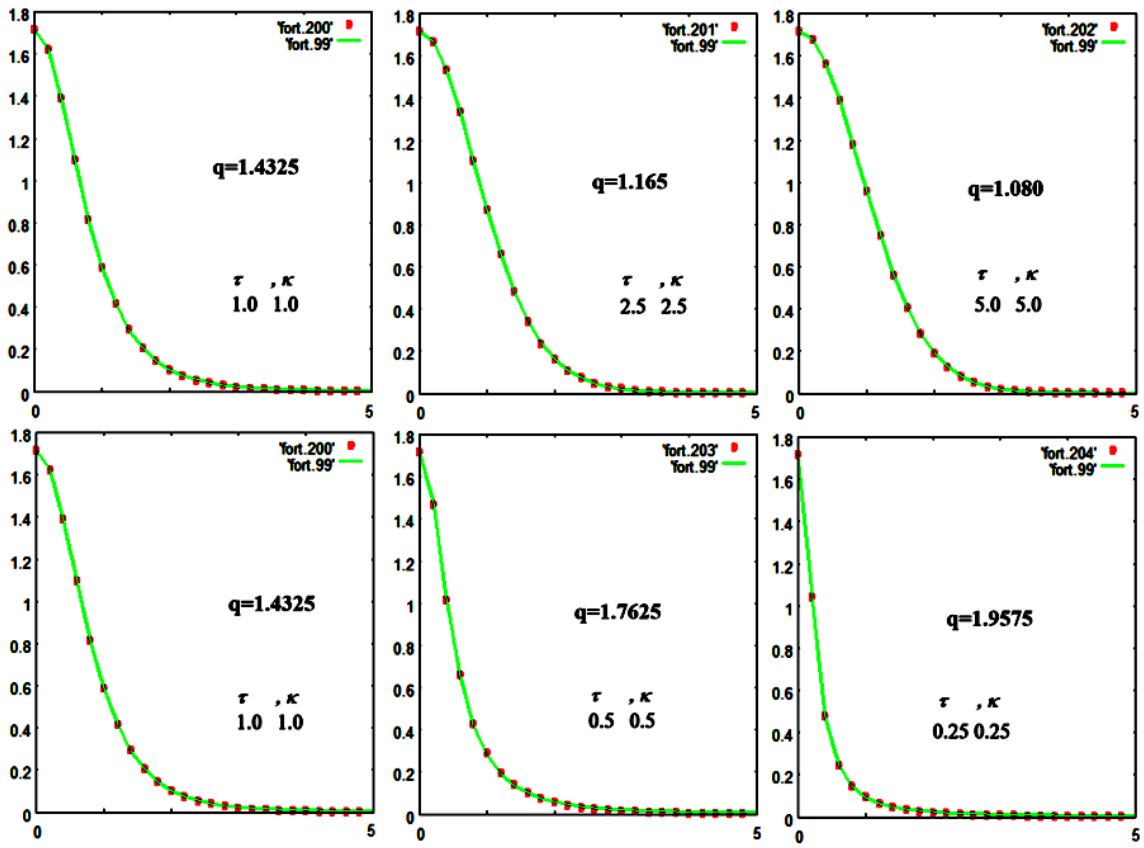

Fig. 5: The Kubo lineshapes of the Figure 4 are represented by red dots. The Kubo lineshapes are compared with q-Gaussian functions. The best fits are given with green lines. The parameters are reported in the plots. They are q-parameter, τ and κ. In the upper part, left panel q=1.4324, τ=1.0, κ=1.0, middle q=1.165, τ=2.5, κ=2.5, right panel q=1.080, τ=5.0, κ=5.0. In the lower part, left panel q=1.4324, τ=1.0, κ=1.0, middle q=1.7625, τ=0.5, κ=0.5, right panel q=1.9575, τ=0.25, κ=0.25 . Note that we pass from a slow Gaussian-like case (q parameter equal to 1.080) to a fast Lorentzian-like case (q parameter equal to 1.9575). The slow and fast cases are compared to the mid case given in the left panels (q parameter1.4325). Plots are given in the linear scale.

Since the difference is very small, the Kubo and q-Gaussian line shapes are giving the same profile in the Figure 5. To appreciate where these functions differ, let us use the semi log scale (Fig.6).

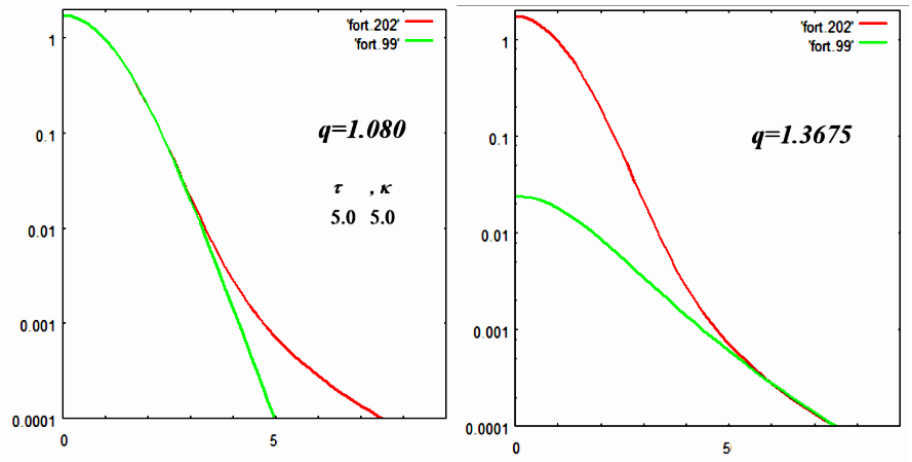

Fig. 6a: Kubo lineshapes in red. The green lines are representing fitted q-Gaussians. For each of the five cases in the Figure 5, we consider on the left, the Kubo and the corresponding q-Gaussian as given by the best fit (Figure 5), proposed here in a semi log scale, and, on the right, the fitted q-Gaussian on the far wings (x greater than 5). The Kubo and the q-Gaussian are differing in their far wings. As before, parameters are q-parameter, τ and κ. Here, in 6a, we see the case characterized by q=1.080, τ=5.0, κ=5.0 (see Fig.5 for the plot given in the linear scale). The panel on the right tells that the wing is characterized by a parameter q=1.3675.

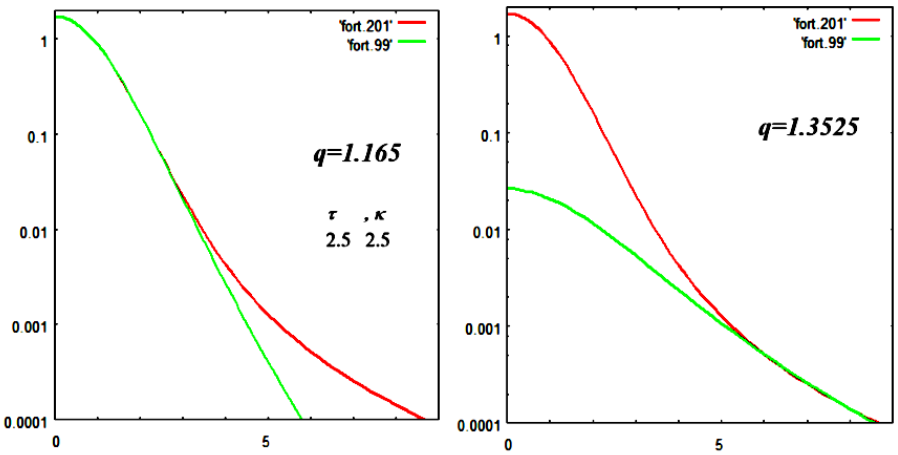

Fig.6b: As in the previous case 6a, we provide the Kubo lineshape in red and q-Gaussian in green. We see the case characterized by q=1.165, τ=2.5, κ=2.5 (see Fig.5 for the plot given in the linear scale). The panel on the right tells that the wing as parameter q=1.3535.

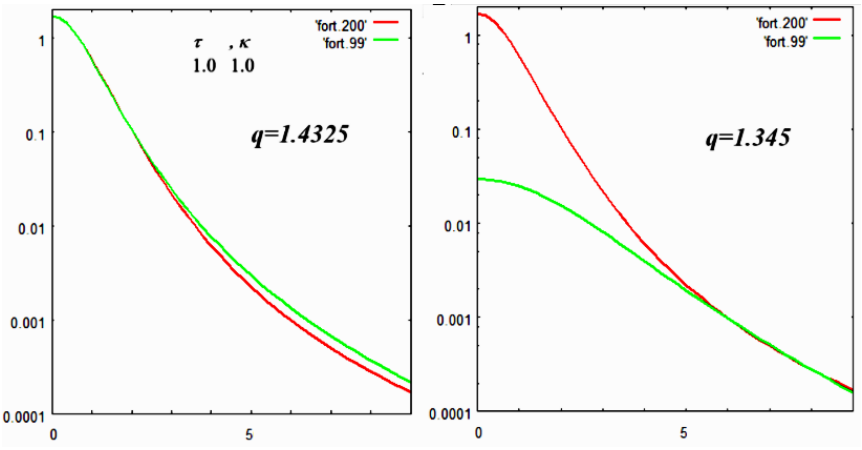

Fig. 6c: Kubo lineshape in red and q-Gaussian in green. We see the case characterized by q=1.4325, τ=1.0, κ=1.0 (see Fig.5 for the plot given in the linear scale). On the right, the wing is shown characterized by parameter q=1.3535.

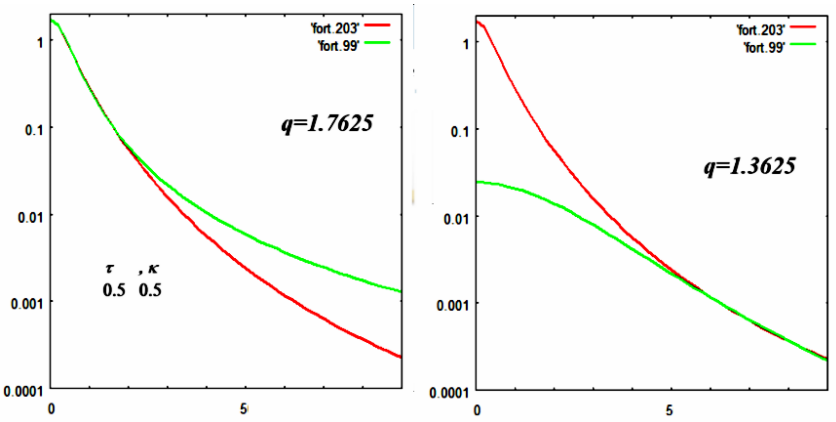

Fig.6d: Kubo lineshape in red and q-Gaussian in green, as in Fig. 6a. The case is q=1.7625, τ=0.5, κ=0.5. Wing has parameter q=1.3625.

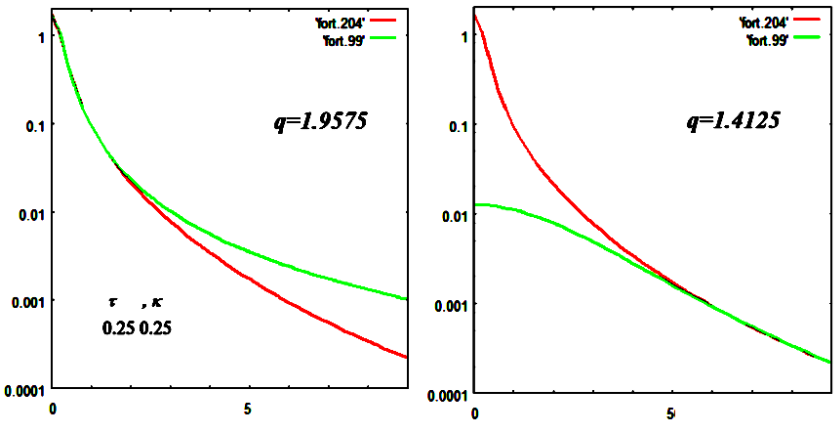

Fig.6e: Kubo lineshape in red and q-Gaussian in green. Parameters are q=1.9575, τ=0.25, κ=0.25. We find the wing with parameter q=1.4125.

From the Figure 6, where the functions are given in the semi log scale (Kubo lineshapes in red and q-Gaussians in green), it is evident that Kubo and q-Gaussians are differing in their far wings. In the five cases here given, the far wings are characterized by q-parameter values ranging from 1.34 to 1.41. It seems that the far wing has a q-parameter increasing its value when the dynamics is becoming faster. As shown by the following Fig.7, in the fast case $\tau_c = 0.05, \kappa = 0.05$, the q-parameter is equal to 2 and the Kubo line shape is almost equal to a Lorentzian function. However, the slow case $\tau_c = 20, \kappa = 20$ does not become a Gaussian profile.

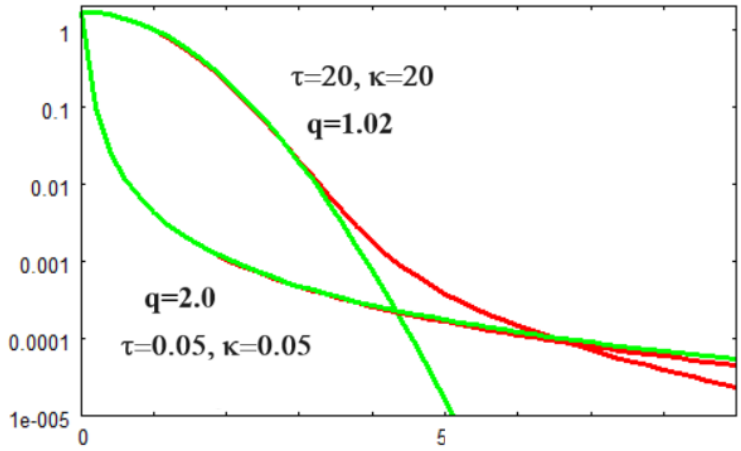

Fig. 7: Kubo line shapes in red and q-Gaussian in green.

Conclusion

The q-Gaussians are able of mimicking the Kubo lineshapes. Only the far-wings are different. The Figures 5-7 are representing how a Kubo lines is passing from a Gaussian-like (slow dynamic) to a Lorentzian-like (fast dynamic) case. However, please note that the far wings have a behavior which is not Gaussian. When processes are very fast, the profile is Lorentzian.

References

1. Dutta, R., Bagchi, K., & Bagchi, B. (2017). Role of quantum coherence in shaping the line shape of an exciton interacting with a spatially and temporally correlated bath. The Journal of Chemical Physics, 146(19).
2. Egelstaff, P. A., & Schofield, P. (1962). On the evaluation of the thermal neutron scattering law. Nuclear Science and Engineering, 12(2), 260-270
3. Feng, Q., & Wilde, R. E. (1988). Vibrational dephasing in aqueous KSCN solution. A memory function and stretched exponential study. Chemical physics letters, 150(6), 424-428.
4. Hanel, R., Thurner, S., & Tsallis, C. (2009). Limit distributions of scale-invariant probabilistic models of correlated random variables with the q-Gaussian as an explicit example. The European Physical Journal B, 72(2), 263.
5. Kirillov, S. A. (1993). Markovian frequency modulation in liquids. Analytical description and comparison with the stretched exponential approach. Chemical physics letters, 202(6), 459-463.
6. Kirillov, S. A. (1999). Time-correlation functions from band-shape fits without Fourier transform. Chemical physics letters, 303(1-2), 37-42.
7. Kirillov, S. A. (2004). Novel approaches in spectroscopy of interparticle interactions. Raman line profiles and dynamics in liquids and glasses. Journal of molecular liquids, 110(1-3), 99-103.
8. Kirillov, S. (2004). Novel approaches in spectroscopy of interparticle interactions. Vibrational line profiles and anomalous non-coincidence effects. In Novel Approaches to the Structure and Dynamics of Liquids: Experiments, Theories and Simulations; Springer: Berlin/Heidelberg, Germany, 2004; pp. 193–227
9. Kubo, R. (1969). A stochastic theory of line shape. Advances in chemical physics, 15, 101-127.
10. Meier, R. J. (2005). On art and science in curve-fitting vibrational spectra. Vibrational spectroscopy, 2(39), 266-269.
11. Naudts, J. (2009). The q-exponential family in statistical physics. Central European Journal of Physics, 7, 405-413.
12. Rothschild, W. G., Perrot, M., & Guillaume, F. (1987). On the vibrational T 2 processes in partially ordered systems. The Journal of chemical physics, 87(12), 7293-7299.
13. Sparavigna, A. C. (2023). The Q(5) Raman Line of Carbon Monoxide and its q-Gaussian Function. Zenodo. https://doi.org/10.5281/zenodo.10396109
14. Sparavigna, A. C. (2022). Entropies and Logarithms. Zenodo. DOI 10.5281/zenodo.7007520
15. Sparavigna, A. C. (2023). q-Gaussian Tsallis Line Shapes and Raman Spectral Bands. International Journal of Sciences, 12(03), 27-40. http://dx.doi.org/10.18483/ijSci.2671
16. Sparavigna, A. C. (2023). q-Gaussian Tsallis Functions and Egelstaff-Schofield Spectral Line Shapes. International Journal of Sciences, 12(03), 47-50. http://dx.doi.org/10.18483/ijSci.2673

17. Sparavigna, A. C. (2023). q-Gaussian Tsallis Line Shapes for Raman Spectroscopy (June 7, 2023). SSRN Electronic Journal. http://dx.doi.org/10.2139/ssrn.4445044
18. Sparavigna, A. C. (2023). Formamide Raman Spectrum and q-Gaussian Tsallis Lines (June 12, 2023). SSRN Electronic Journal. http://dx.doi.org/10.2139/ssrn.4451881
19. Sparavigna, A. C. (2023). Tsallis and Kaniadakis Gaussian functions, applied to the analysis of Diamond Raman spectrum, and compared with Pseudo-Voigt functions. Zenodo. https://doi.org/10.5281/zenodo.8087464
20. Sparavigna A. C. (2023). Tsallis q-Gaussian function as fitting lineshape for Graphite Raman bands. ChemRxiv. Cambridge: Cambridge Open Engage; 2023.
21. Sparavigna A. C. (2003). Fitting q-Gaussians onto Anatase TiO2 Raman Bands. ChemRxiv. Cambridge: Cambridge Open Engage; 2023.
22. Sparavigna, A. C. (2023). SERS Spectral Bands of L-Cysteine, Cysteamine and Homocysteine Fitted by Tsallis q-Gaussian Functions. International Journal of Sciences, 12(09), 14–24. https://doi.org/10.18483/ijsci.2721
23. Sparavigna, A. C. (2023). Asymmetric q-Gaussian functions to fit the Raman LO mode band in Silicon Carbide. ChemRxiv. Cambridge Open Engage; 2023.
24. Sparavigna, A. C. (2023). Generalizing asymmetric and pseudo-Voigt functions by means of q-Gaussian Tsallis functions to analyze the wings of Raman spectral bands. ChemRxiv, Cambridge Open Engage, 2023.
25. Sparavigna, A. C. (2023). Convolution and Fourier Transform: from Gaussian and Lorentzian Functions to q-Gaussian Tsallis Functions. International Journal of Sciences, 12(11), 7-11.
26. Tagliaferro, A., Rovere, M., Padovano, E., Bartoli, M., & Giorcelli, M. (2020). Introducing the novel mixed gaussian-lorentzian lineshape in the analysis of the raman signal of biochar. Nanomaterials, 10(9), 1748.
27. Tokmakoff, A. (2009). MIT Dept. of Chemistry, Lecture Notes, Archive
28. Townsend, R. (2008). Astronomy 310, Stellar Astrophysics, Fall Semester 2008, Lecture Notes, Archive
29. Tsallis, C. (1988). Possible generalization of Boltzmann-Gibbs statistics. Journal of statistical physics, 52, 479-487.
30. Tsallis, C. (1995). Some comments on Boltzmann-Gibbs statistical mechanics. Chaos, Solitons & Fractals, 6, 539-559.
31. Tsallis, C. (2023). Senses along Which the Entropy Sq Is Unique. Entropy, 25(5), 743.
32. Umarov, S., Tsallis, C., Steinberg, S. (2008). On a q-Central Limit Theorem Consistent with Nonextensive Statistical Mechanics. Milan J. Math. Birkhauser Verlag. 76: 307–328. doi:10.1007/s00032-008-0087-y. S2CID 55967725.